

SINGLE-FEEDING CIRCULARLY POLARIZED TM_{21} -MODE ANNULAR-RING MICROSTRIP ANTENNA FOR MOBILE SATELLITE COMMUNICATION

X. Chen, G. Fu, S. X. Gong, Y. L. Yan, and Z. Y. Zhang

National Key Laboratory of Antennas and Microware Technology
Xidian University, Xi'an 710071, China

Abstract—A novel TM_{21} -mode circularly polarized (CP) annular-ring microstrip antenna (ARMSA) is presented. The annular ring is designed working at TM_{21} mode, and conical radiation pattern is obtained. At the inner of annular ring, a simple ring-shaped feeding line is arranged to implement impedance matching and CP operation. Therefore, the antenna has good impedance and CP performance, as well as a compact structure. The measured results indicate that the antenna has high low-elevation gains and omnidirectional azimuth coverage. The peak gain reaches 4.3 dBic at elevation angle of 47° , and in the range of 10° – 70° , the gain is above 0 dBic. The impedance bandwidth for $S_{11} \leq -10$ dB is 2.3% at 1.601 GHz. The proposed antenna can be used in mobile earth-station equipment for satellite positioning and communication systems in global or local.

1. INTRODUCTION

In the applications of satellite communication, the mobile terminal antennas are demanded strictly in physical configurations and electronic performances. Circularly polarized (CP) microstrip antennas are widely used in this field with the advantages of low profile and good characteristics [1–3]. Rectangular patch [1, 2] and circular patch [3] are two most conventional microstrip configurations. In recent years, annular-ring microstrip antenna (ARMSA) has been widely investigated because of its some advantages [4–9]. It can be seen as cutting a concentric circular slot on a circular patch. At a fixed operating frequency, an annular-ring patch has smaller dimensions than a circular patch; it is because the behavior of slotting on the

patch extends the flowing path of the surface current [4]. The feature can be used in arranging antenna array. However, the large input impedance of TM_{11} -mode ARMSA is an obstacle of its applications. Up to now, several techniques have been presented to partly overcome the obstacle: 1) the impedance-transformer line feeding [5]; 2) the electromagnetic coupling feeding [6, 7]; 3) the aperture coupling feeding [8]; and 4) adding parasitic patch [4]. Comparing with the traditional microstrip antennas, the realization of circular polarization of ARMSA also refers to two approaches: introducing perturbation segments [5, 7], and adopting two feeding points [4, 9]. The methods of perturbation segments have simple structure but narrow bandwidth. Large bandwidth can be obtained through two feeding points with equal amplitude and 90° difference, but additional feeding network is demanded.

As well known, the TM_{11} -mode microstrip antenna has the maximum gain along the normal of the patch, i.e., at zenith, and the gains close to horizon drop quickly [3, 4]. For mobile terminals of satellite communication, it is needed the antenna has good and uniform radiation characteristics in the whole upper half space, especially at low elevation in some cases. In the application of geostationary satellite communication, if the mobile earth terminals lie in the mid- and high-latitude district, the antennas should have good omnidirectional low-elevation gains. The gains at zenith could be sacrificed partially. Presently, there are mainly two approaches for microstrip antennas to improve low-elevation gains: one is adapting high-dielectric substrate with large thickness to increase surface wave radiation in horizon; 2) another is reshaping the radiation patch or the ground to enhance the radiation at low elevation [10]. Both types mainly work at TM_{11} mode, and the improvement of low-elevation gains is limited. Furthermore, the low-profile features may be discarded. A potential candidate is TM_{21} -mode microstrip antenna, which has omnidirectional conical radiation pattern with good low-elevation gains [11]. TM_{21} -mode ARMSAs also have the conical radiation pattern as well as the small sizes, but it also has the problem of large input impedance. Presently, the proposed TM_{21} -mode ARMSAs work at linear polarization [12, 13], which are unsuitable to the applications of satellite communication.

In this paper, we present a novel CP TM_{21} -mode ARMSA. Making use of the inner space of the annular ring, a simple feeding ring is arranged at the inner of the annular ring to realize the circular polarization and solve the problem of impedance matching. Therefore, the antenna has a compact feature with single feeding point. In part 2 of the paper, the antenna configuration and design methodology will be shown, and the experimental results and discussions will be given

in part 3.

2. ANTENNA CONFIGURATION AND DESIGN

Figure 1 shows the geometry of the proposed CP TM_{21} -mode ARMSA. The annular ring and the feeding line are connected directly and etched together on the top surface of a 4 mm-thick substrate with $\epsilon_r = 2.55$. The function of the annular ring is to build resonance of TM_{21} -mode and radiate energy efficiently, and that of the feeding line is to provide CP feeding and match with 50Ω port. The sizes of the annular ring are determined by the resonant frequency of the specified mode and the input impedance of the ring at the frequency. When the annular-ring patch operates at TM_{21} mode, the surface current on the patch is sketched in solid line in Figure 2(a). An arrow line means about a half guided wavelength, so the average perimeter of the ring is approximately $2\lambda_{21}$ in effective permittivity. Its expression is shown as (1). Therefore, the resonant frequency can be expressed as (2).

$$\pi(a + b) = \frac{2\lambda_0}{\sqrt{\epsilon_e}} = \frac{2c}{f_{21} \cdot \sqrt{\epsilon_e}} \tag{1}$$

$$f_{21} = \frac{2c}{\pi(a + b) \cdot \sqrt{\epsilon_e}} \tag{2}$$

where a and b are the inner radius and outer radius separately, $\pi(a + b)$ can be seen as the the average perimeter of the ring, the λ_0 is the

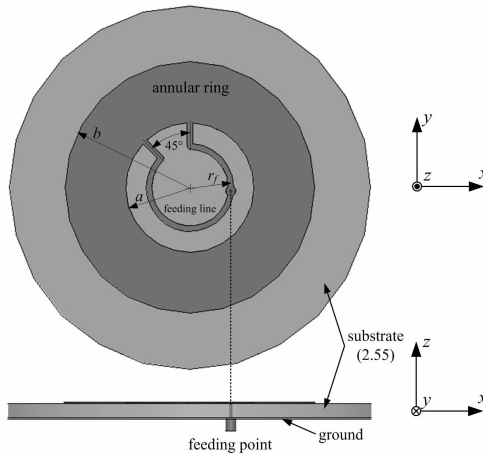


Figure 1. Geometry of proposed CP annular-ring microstrip antenna.

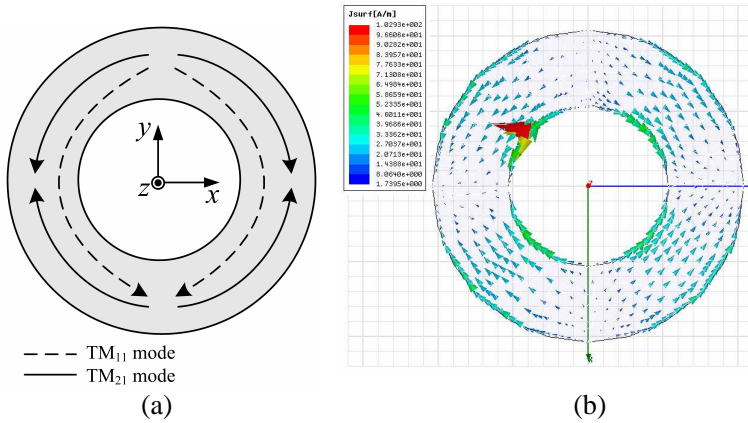


Figure 2. Current distribution on annular ring. (a) Sketch map of surface current. (b) Simulated current of TM₂₁ mode.

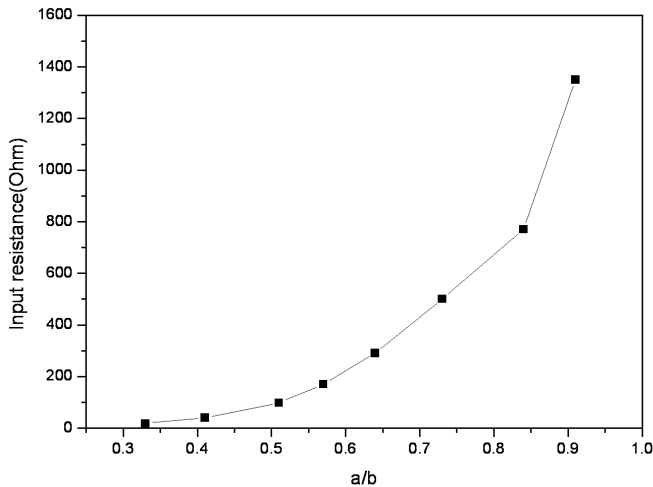


Figure 3. Simulated input resistance of the ring versus a/b .

wavelength in air, ϵ_e is the effective permittivity around the ring, c is the speed of light, f_{21} and λ_{21} are the operating frequency and wavelength of TM₂₁ mode. In addition, the ratio of a and b (a/b) controls the input impedance greatly. Figure 3 shows the simulated input resistance at the inside boundary of the annular ring versus a/b at the given resonant frequency 1.601 GHz. It is worth noting that smaller input impedance can be acquired at inside boundary than at

outside boundary. Obviously, as a/b increases, the input resistance rises quickly. It shows $50\ \Omega$ matching is hard to obtain with a narrow annular ring. However, we can get $100\ \Omega$ -input impedance to match with $100\ \Omega$ microstrip line when a/b is about 0.5. It is useful to us to design a simple CP feeding network later. Thus, through the refined simulation, a and b is determined as 26.7 mm ($0.14\lambda_0$) and 51.9 mm ($0.277\lambda_0$) separately.

The feeding line is designed to match with $100\ \Omega$ impedance. The ring-shaped feeding line is arranged at inner of the annular ring for a compact structure. The radius r_f of the feeding ring is 17 mm for 90° difference, and the width of the line is 2.3 mm for $100\ \Omega$ characteristic impedance. Therefore, without the impedance-transformer line, $50\ \Omega$ input impedance is acquired at feeding point by the simple parallel feeding structure. Adjusting the position of the feeding point along the feeding ring, we can obtain two equal-amplitude and 90° -difference excitations accurately. To excite TM_{21} mode on the annular ring, the angular spacing between two excitations should be 45° [11]. A metallic ground is attached to the bottom of the substrate for semi-space radiation coverage.

3. RESULTS AND DISCUSSIONS

A prototype is fabricated. Figure 4 is the photo of the prototype. Both radii of the substrate and ground are fixed at 75 mm ($0.4\lambda_0$) for a suitable antenna size. The impedance performance is measured by the HP network analyzer 8753D, and the simulated results are carried out by HFSS 11. Figure 5 shows the measured return loss comparing with the simulated one. The two curves agree very well. In terms of the data, the measured impedance bandwidth for $S_{11} \leq -10$ dB is 37 MHz, ranging from 1.586 GHz to 1.623 GHz. The relative bandwidth is 2.3%



Figure 4. Photo of the prototype.

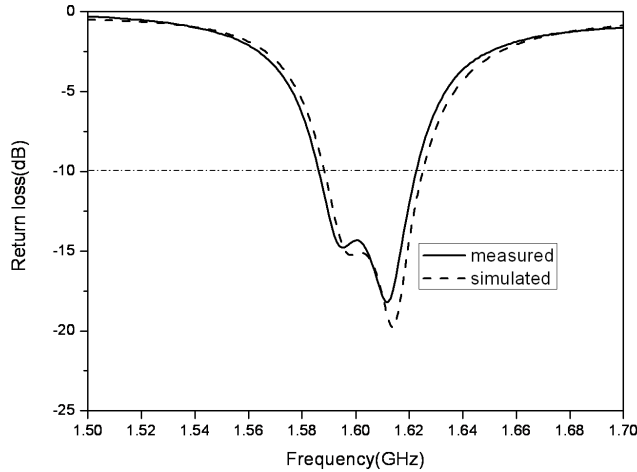


Figure 5. Measured and simulated return loss.

at operating frequency 1.601 GHz. The bandwidth is not wide, but it is enough for the satellite communication service with low information capacity, e.g., satellite position service and short message service [10].

The radiation patterns (RP), the gains, and the axial ratio (AR) followed are all measured through the amplitude-phase method, i.e., these performances are obtained through the measurements of the amplitude and phase of two linearly polarized sections in two orthogonal directions. Figure 6 shows the CP gain RP of the prototype in two main planes at 1.601 GHz. The left hand circular polarization (LHCP) and right hand circular polarization (RHCP) are both displayed in the figures. The both polarizations display the conical RP. Because of the existence of ground, the radiation energy is mainly centralized in RHCP. From the measured values, the peak gain reaches 4.3 dBic at 43° away from zenith (elevation angle of 47°), and in the range of 20° – 80° away from zenith (elevation angles of 10° – 70°), the gains are more than 0 dBic. It shows the TM_{21} -mode ARMSAs have lower radiation elevation than that of TM_{21} -mode circular microstrip antennas, whose peak gain lies about 35° away from zenith (elevation angles of 55°) [11].

In terms of its performances, the proposed antenna is very suitable for the mobile earth terminals in geostationary satellite communication applications. For example, the most area of China is located in the range of 20° N to 55° N. According to the geometry between geostationary satellites and earth terminals, shown as in Figure 7, the

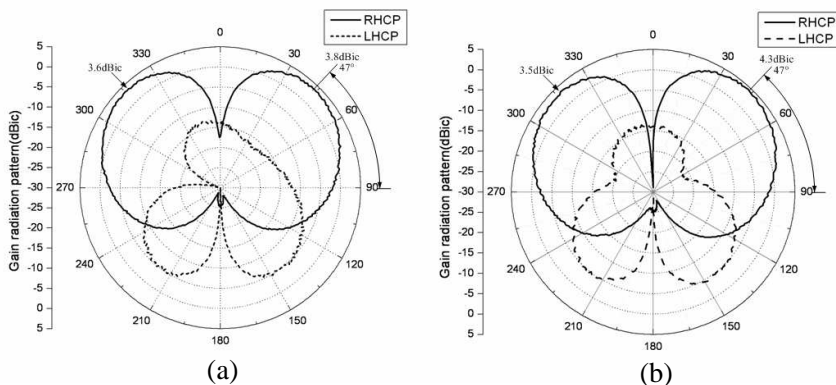


Figure 6. Measured radiation patterns at 1.601 GHz. (a) In x - z plane. (b) In y - z plane. — RHCP patterns, - - - LHCP patterns.

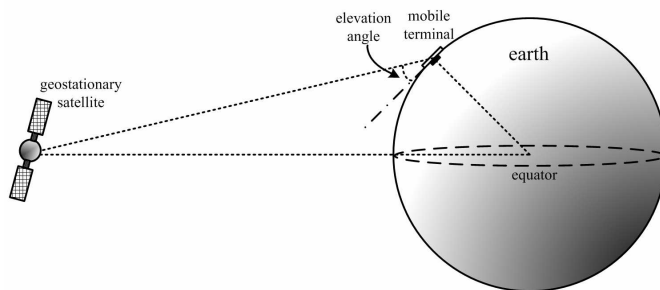


Figure 7. Sketch of the mobile terminal and geostationary satellite.

antennas on mobile terminals should radiate well in the elevation angles of 27° – 67° . In this range, the proposed antenna has more than 1.5 dBic gains. For the most mid- and high-latitude countries and regions, the proposed antenna could also be employed. In addition, it also can be seen as a wide-beamwidth antenna in a way. Summing up the two-side ranges for gain ≥ 0 dBic, it is about 120° , and the peak gain reaches 4.3 dBic at lean. The performances are better than those of wide-beamwidth TM_{11} -mode microstrip antenna [10]. Although the proposed RP is null at zenith, in terms of the positioning theory of GPS, the satellite signal from the direction of low elevation contributes mostly to the positioning precision. So the proposed antenna is also useful to the applications of Global Navigation satellite systems (GNSS).

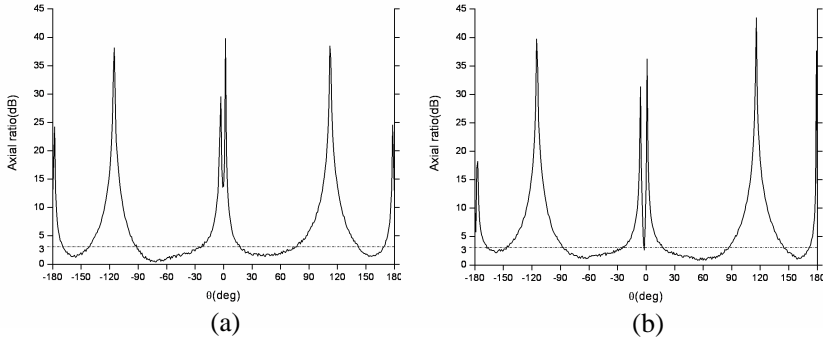


Figure 8. Measured axial ratio patterns. (a) In x - z plane. (b) In y - z plane.

In radiation patterns, it is noted the RHCP pattern in y - z plane is not symmetrical as that in x - z plane. In y - z plane, the gain at -43° (317°) is 3.5 dBic while the gain is 4.3 dBic at 43° . But in x - z plane, the gain is 3.6 dBic and 3.8 dBic separately at two sides. The main reason is shown in Figure 2. While the TM_{21} mode is excited on the ring, the undesired mode, i.e., TM_{11} mode, is also aroused. It makes the total current distribution unbalanced along y -axis but not along x -axis.

For satellite communication antennas, the AR is a key technical specification. The low LHCP components indicate the proposed antenna has high cross polarization discriminations (XPD). It can reduce the effect of depolarization greatly when the electromagnetic wave is converted by the rain or the multi-path effect in propagation. Figure 8 shows the AR patterns separately in x - z plane and y - z plane. The AR is below 3 dB in the range of 25° – 80° away from zenith (elevation angles of 10° – 65°). It is worth noting that the good AR at low elevation can reduce the interference from the multi-path effect near ground. It can improve the signal quality of the satellite communications.

4. CONCLUSION

A novel TM_{21} -mode CP ARMSA with simple structure is proposed and studied in this paper. The ring-shaped feeding line can provide good impedance matching and CP performance for annular ring, and the feeding line is designed carefully at the inner of the ring. The measured results indicate that the proposed antenna has the peak

gain (4.3 dBic) at elevation angle of 47° and omnidirectional azimuth coverage. The feature is suitable for mobile earth-station equipment of satellite positioning and communication systems in global or local. In the future work, multiple-feed-points technique will be considered and investigated to suppress the undesired modes.

REFERENCES

1. Heidari, A. A., M. Heyrani, and M. Nakhkash, "A dual-band circularly polarized stub loaded microstrip patch antenna for GPS applications," *Progress In Electromagnetics Research*, Vol. 92, 195–208, 2009.
2. Yang, S. S., K.-F. Lee, A. A. Kishk, and K.-M. Luk, "Design and study of wideband single feed circularly polarized microstrip antennas," *Progress In Electromagnetics Research*, Vol. 80, 45–61, 2008.
3. Liao, W. and Q.-X. Chu, "Dual-band circularly polarized microstrip antenna with small frequency ratio," *Progress In Electromagnetics Research Letters*, Vol. 15, 145–152, 2010.
4. Chen, X., G. Fu, S.-X. Gong, et al., "Circularly polarized stacked annular-ring microstrip antenna with integrated feeding network for UHF RFID readers," *IEEE Antennas Wireless Propag. Lett.*, Vol. 9, 542–545, 2010.
5. Chen, H. M. and K. L. Wong, "On the circular polarization operation of annular-ring microstrip antenna," *IEEE Trans. Antennas Propag.*, Vol. 47, No. 8, 1289–1292, 1999.
6. Row, J. S., "Dual-frequency circularly polarised annular-ring microstrip antenna," *Electron. Lett.*, Vol. 40, No. 3, 153–154, 2004.
7. Lin, Y. F., H. M. Chen, and S. C. Lin, "A new coupling mechanism for circularly polarized annular-ring patch antenna," *IEEE Trans. Antennas Propag.*, Vol. 56, No. 1, 11–15, 2008.
8. Row, J. S., "Design of aperture-coupled annular-ring microstrip antennas for circular polarization," *IEEE Trans. Antennas Propag.*, Vol. 53, No. 5, 1779–1784, 2005.
9. Guo, Y. X., L. Bian, and X. Q. Shi, "Broadband circularly polarized annular-ring microstrip antenna," *IEEE Trans. Antennas Propag.*, Vol. 56, No. 1, 2474–2477, 2009.
10. Su, C. W., S. K. Huang, and C. H. Lee, "CP microstrip antenna with wide beamwidth for GPS band application," *Electron. Lett.*, Vol. 43, No. 20, 1062–1063, 2007.
11. Hang, J., "Circularly polarized conical patterns from circular

- microstrip antennas,” *IEEE Trans. Antennas Propag.*, Vol. 32, No. 9, 991–994, 1984.
12. Lin, S. Y. and K. L. Wong, “A conical-pattern annular-ring microstrip antenna with a photonic bandgap ground plane,” *Microw. Opt. Technol. Lett.*, Vol. 30, No. 3, 159–161, 2001.
 13. Lin, S. Y. and K. C. Huang, “A compact microstrip antenna for GPS and DCS application,” *IEEE Trans. Antennas Propag.*, Vol. 53, No. 3, 1227–1229, 2005.